

CHAPTER 5 – TEST PROTOCOL

As indicated before, the five-step procedure for quality management of the ACP was adapted for evaluating the modulus of the ACP layer in situ. The procedure followed here can be summarized in the following five steps:

1. Selection and Marking of Test Sites.
2. Conducting PSPA Tests.
3. Retrieval of Cores.
4. Conducting Lab Tests.
5. Relating Lab and Field Test Results.

Each step is described below. The results from one actual site, Taylor River Road, are also used to clarify the process.

SELECTION AND MARKING OF TEST SITES

At each site, the first step consisted of visually inspecting the pavement and selecting a test section. The main criteria for selecting the site were safety of the crew and reasonable uniformity of the section.

About 30 points were marked on the pavement as depicted in Figure 16. Of these points, fifteen were located in the wheel path and fifteen along the midlane of the road.

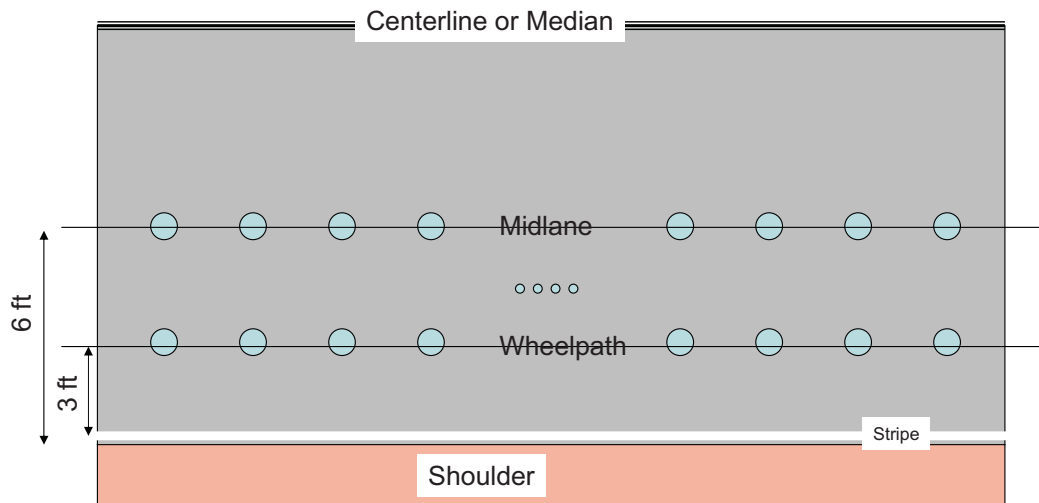


Figure 16. Schematic. Typical Marking of Sites.

PSPA TESTS

Each of the thirty points was tested with the PSPA four times, twice with the instrument oriented parallel to the centerline and twice perpendicular. Repeating the test at each point will provide information about the repeatability of the device as well as the variation in the properties in the two perpendicular directions due to the compaction pattern and the damage to the pavement. At each point, the temperature of the pavement was also measured with an infrared gun in addition to the thermistor measurement made by the PSPA.

A typical waveform collected at one point with the PSPA software is shown in Figure 17. Three time records are shown in the figure. The red record is the time history of the sensor placed in the source, with the amplitude heavily attenuated. This record is useful to the advanced user for ensuring that the source is functioning properly. Additionally, the record is used in the impact-echo analysis.

The black record depicts the time history as recorded by the sensor closer to the source (near receiver), and the green record is the time history from the far sensor. These two records are used in the determination of the modulus with the USW method. Both records demonstrate the typical arrival of the surface energy as depicted by the full sine-wave cycle in the left hand of the records, after which the energy attenuates rapidly. On the left side of the figure, under the “Results” section, the modulus obtained for this section (i.e. 1630 ksi) is presented as soon as the data collection is completed.

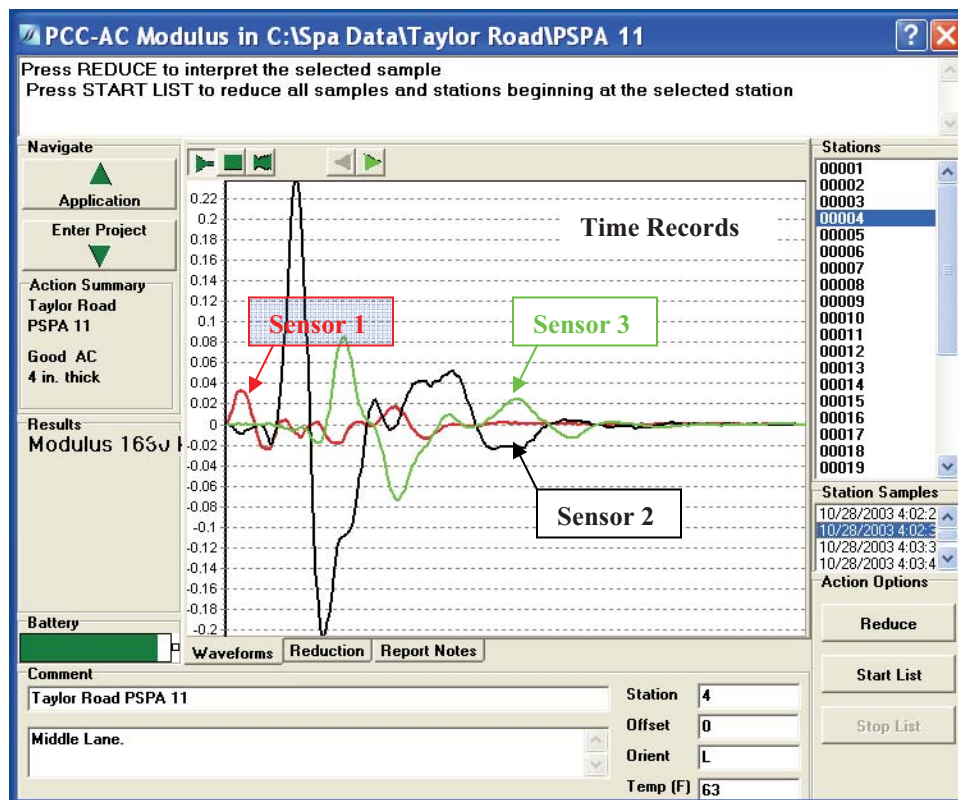


Figure 17. Screen Shot. Typical Time Records as Demonstrated by PSPA Software.

In the next step, the operator has the option of viewing the reduced data, as shown in Figure 18. Several items can be inspected in the figure. The graph at the bottom is the phase spectrum (a variation in phase delay due to propagation of wave with frequency). This is the intermediate result obtained from the analysis of the time records shown in Figure 17. As described in Nazarian et al. (1997), this curve should represent a saw-tooth pattern as it does in the figure. The green record is the measured phase spectrum and the red one is the best fit to the data by the software. The two curves follow one another quite well.

The upper graph labeled “Dispersion Curve is a representation of the variation in modulus (horizontal axis) with wavelength (vertical axis). As indicated before, for shorter wavelengths, the wavelength approximates the thickness of the layer. For this reason, the vertical axis is labeled as thickness. The dispersion curve, which is directly calculated from the phase spectrum, is represented by green dots. The red vertical solid line in this graph corresponds to the range of thickness along which the average modulus is calculated. This average value is the number shown in the “Results” section (i.e., 1630 ksi). The shortest thickness is controlled by the spacing between the receivers, the top size aggregate of the mixture and the shortest wavelengths measured by the PSPA at this transducer spacing. The longest thickness is input by the user as a nominal value. In this case the nominal thickness and the actual thickness of the layer coincide quite well, as the measured dispersion curve is uniform up to a thickness of 4 in. beyond which the curve breaks towards lower moduli.

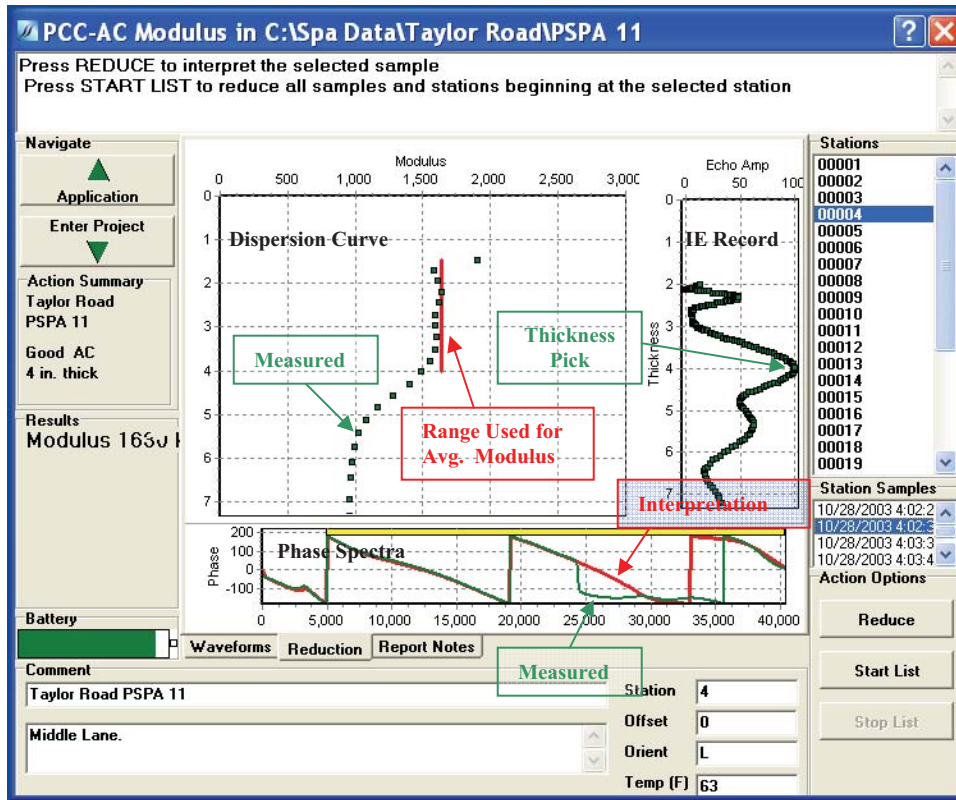


Figure 18. Screen Shot. Typical Interpreted Results as Demonstrated by PSPA Software.

On the right hand side of the graphs, the impact-echo results are shown. The most probable thickness corresponds to the pick of the curve as marked. Even though in this case, the results are quite close to the actual thickness, at this time this methodology will not provide consistent results on ACP layers. We feel that the change in the slope of the dispersion curve may be a better indicator of the thickness, especially in multi-course pavements.

The variations in seismic moduli along the wheel path and the midlane at this site are shown in Figure 19. For each test point, four numbers, corresponding to the four measurements, are shown. The two individual measurements corresponding to either the longitudinal or perpendicular measurements are almost always within 5% of one another. In some cases, the results from the two directions are different indicating heterogeneity of the material due to the compaction pattern, due to localized segregation, or due to load or environmental induced micro-cracking or cracking of the ACP. Hugo et al. (1997) have well documented this phenomenon. Six red circles in the figure correspond to the core locations.

The temperature varied from location to location. The temperature measured at each site was used to adjust the AC moduli to 77°F. The relationship suggested by Li and Nazarian (1994) for adjusting the modulus of AC to a reference temperature of 25° C (77° F) was used here. That relationship is in the form of

$$E_{25} = E_t / (1.35 - 0.014 t) \quad (4.11)$$

where E_{25} and E_t are the moduli at 25° C and temperature t (in Celsius). A temperature gun was used to measure the temperature at each test point. This relationship is approximate, but in the absence of data for developing temperature-modulus relationships, it was used in this study.

The measured seismic moduli along this site vary from a low of about 1600 ksi close to Station 1 to a high of about 2200 ksi towards the end of the tested section. To validate these variations, cores were retrieved and tested as discussed in the next section.

RETRIEVAL OF CORES

At each site six cores were retrieved, three along the wheel path and three along the midlane. In order to core in a systematic manner, the results from the PSPA were inspected in the field. The locations with the highest modulus and lowest modulus, as well as a location with an approximately average modulus were identified and cored. A picture of the coring operation is shown in Figure 20. The CFLHD staff kindly performed all the coring. The cores were clearly labeled, air-dried and packaged for shipment to El Paso for laboratory testing.

As soon as the cores were received in the laboratory, they were re-labeled, and the ends in contact with the base were saw-cut to obtain smooth ends. The cores as received in the lab and after saw-cut are shown in Figure 21.

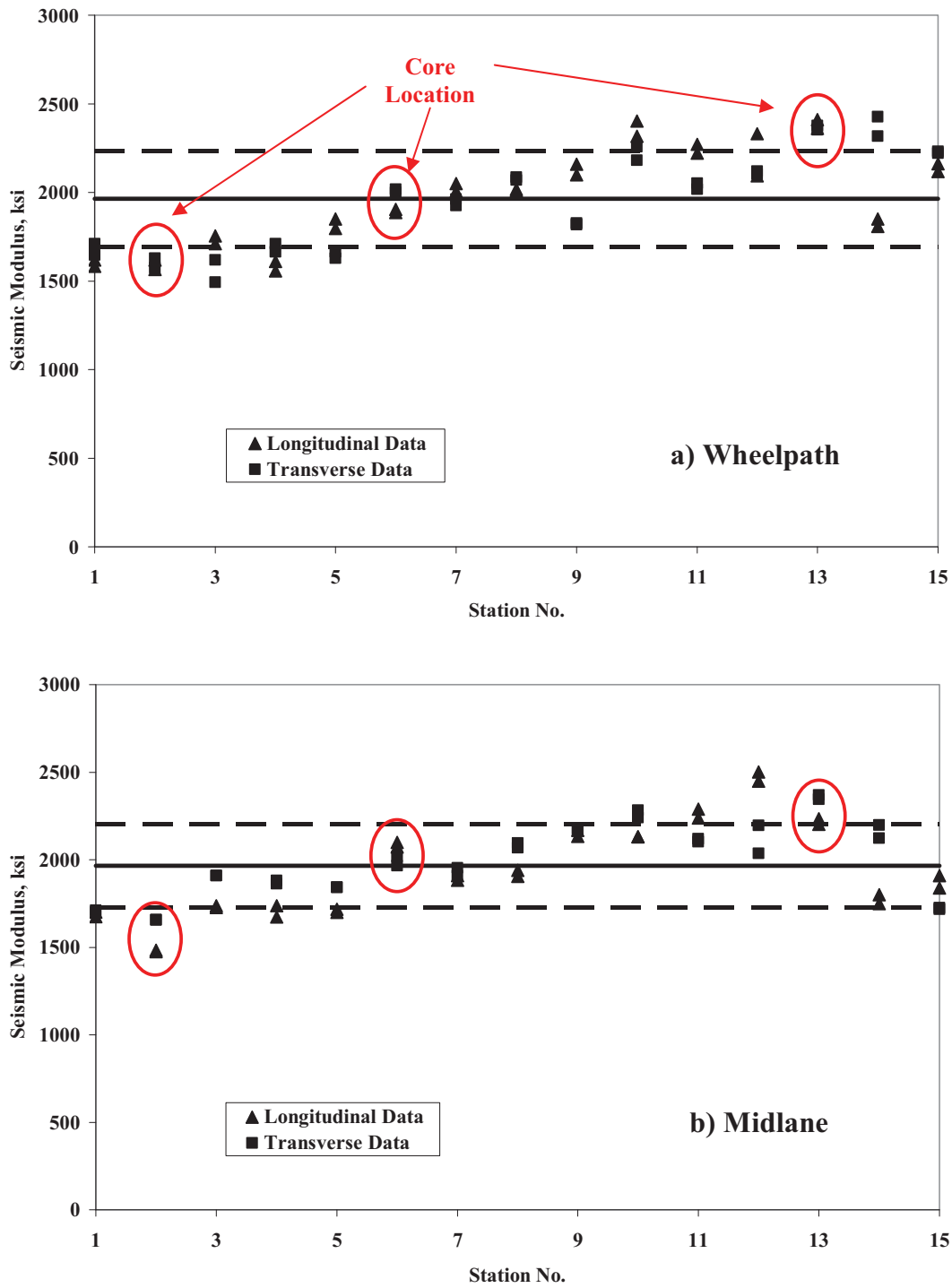


Figure 19. Graph. Typical Variation in Modulus along a Site.



Figure 20. Photo. Typical Coring Operation by CFLHD Staff.



Figure 21. Photo. Typical Cored Retrieved from the Site.

LAB TESTS

In this step, the six cores were tested at room temperature with the ultrasonic device shown in Figure 12 to determine their seismic moduli. Two to four specimens for each site were then subjected to the diametral resilient modulus tests as described in Chapter 4.

After the completion of the resilient modulus tests, the cores were then used to determine the volumetric properties of the specimens. The first step consisted of determining the air void content of the specimens. The specimens that underwent resilient modulus testing experienced excess deformation and could not be used for air void determination. Therefore, air voids were only determined for specimens that were not subjected to lab tests.

In the next step, the asphalt content of the material was determined using the NCAT ignition oven. In that test method, the specimen is placed in an oven for an extended period of time to burn the binder. The remaining aggregates after ignition oven test were sieved to obtain the gradation of the aggregates from each core.

The results from this activity for the site used as an example are included in Table 1. The asphalt content is reasonably uniform and the gradation is fairly similar. The voids in total mix (VTM), however, vary by about 1.5% between the two cores tested. As expected, the higher VTM is associated with the specimen with the lower modulus.

Table 1. Volumetric Information from Cores Retrieved from the Site.

Sample ID	AC Content	Voids in Total Mix	Modulus with Ultrasonic Device, ksi	Gradation (Percent Passing)						
				1/2 in.	3/8 in.	No. 4	No. 10	No. 40	No. 80	No. 200
1	6.2%	--	2142	97.9	83.3	53.7	30.6	13.5	7.9	3.0
2	6.1%	--	2177	100.0	82.3	52.8	31.6	14.5	8.6	4.2
3	5.6%	--	2286	98.7	74.9	45.9	28.7	13.5	8.0	3.7
4	6.2%	--	2312	100.0	83.6	53.3	30.9	14.2	9.1	4.2
5	--	6.13%	2058	--	--	--	--	--	--	--
6	--	4.77%	2275	--	--	--	--	--	--	--
Average	6.0%	5.45%	2208	99.2	81.0	51.4	30.4	13.9	8.4	3.8
COV	5%	17.6%	4.5%	1%	5%	7%	4%	4%	7%	15%

RELATING LAB AND FIELD TEST RESULTS

The results from the PSPA, ultrasonic lab device and resilient modulus tests are combined to obtain the master curve as described in Chapter 4. This curve can then be used to obtain the desired modulus for structural design of pavement.

A typical master curve is shown in Figure 22. As indicated before, the resilient modulus tests were carried out at three temperatures. The “reduced” or shifted data points are shown in the

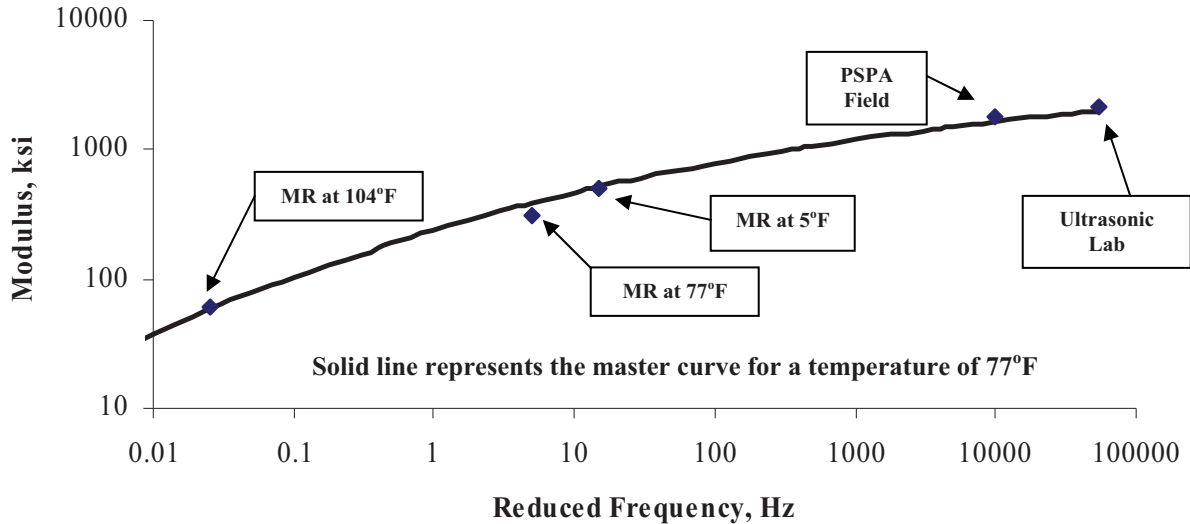


Figure 22. Graph. Typical Master Curve to Combine all Test Results.

figure. The number of data points from diametral resilient modulus tests, unlike from dynamic modulus tests shown in Figure 5, is limited. This is a limitation of the diametral resilient modulus test. As indicated before, it would have been desirable to conduct dynamic modulus tests on these specimens to get a complete master curve. Because of the length-to-diameter restrictions, this was not possible. For this example, the design modulus at a frequency of 15Hz is about 514 ksi while the PSPA modulus is about 2150 ksi.

In the next step the moduli from the ultrasonic tests on the cores and the PSPA were compared. Typical results from this activity are included in Figure 23. In this case, the two results are within 20% of one another. The reasons for the differences, aside from any errors in measurements and analyses, are the following.

- The use of approximate temperature correction method for converting the field modulus to lab modulus. As indicated in Chapter 3, modulus-temperature relationships could have been established in the laboratory if more material was available.
- The measurements with the PSPA are impacted by the micro-cracking and internal damage of the specimen, while the lab tests primarily characterize the material properties.
- Approximations due to the assumption of mass density and/or Poisson's ratio in the determination of moduli

It should be mentioned that the cores from the average modulus position on each pavement section were used for determining the density and Poisson's ratio.

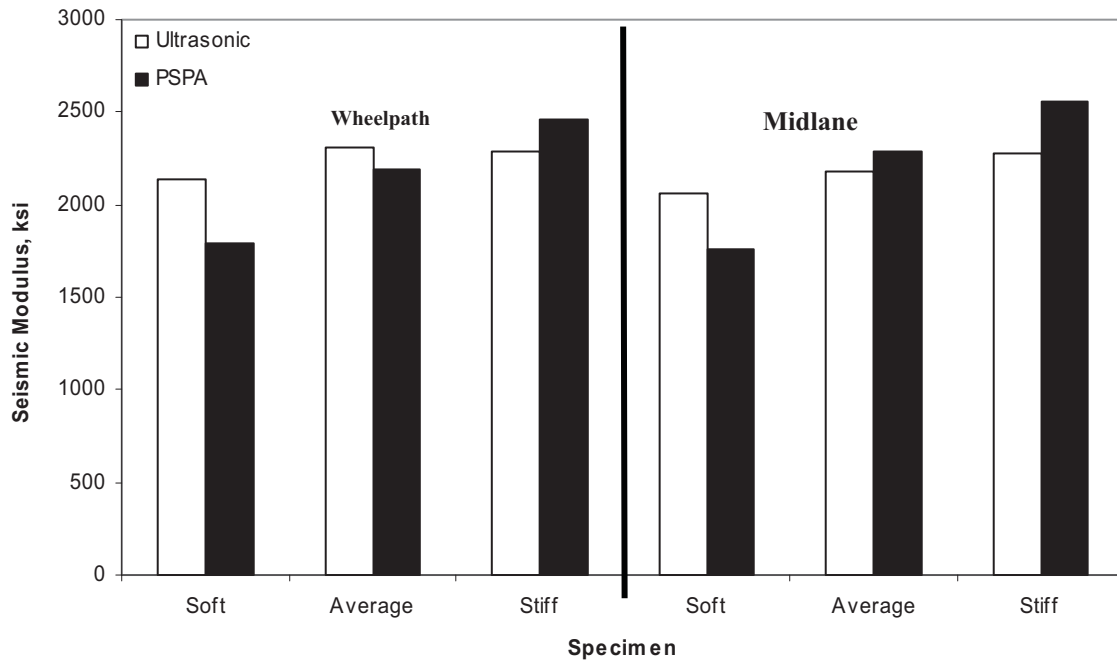


Figure 23. Graph. Typical Comparison of PSPA Field Moduli with Ultrasonic Lab Results.

